2007

Cylindrical quasi-cavity waveguide for static wide angle pattern projection

Kaveh Sahba
Edith Cowan University

Kamal Alameh
Edith Cowan University

Clifton Smith
Edith Cowan University

Arie Paap

10.1364/OE.15.003023

Cylindrical quasi-cavity waveguide for static wide angle pattern projection

Kaveh Sahba[1], Kamal E. Alameh[1], Clifton L. Smith[2], and Arie Paap[1]

[1]*WA Centre of Excellence for MicroPhotonic Systems, Electron Science Research Institute, Edith Cowan University, 100 Joondalup Drive, Joondalup 6027, Western Australia*

[2]*School of Engineering and Mathematics, Edith Cowan University, 100 Joondalup Drive, Joondalup 6027, Western Australia*

k.sahba@ecu.edu.au, a.paap@ecu.edu.au, k.alameh@ecu.edu.au, clifton.smith@ecu.edu.au

http://comps.ecu.edu.au

Abstract: Beam deflection methods such as rotary mirrors and motorized turning optical heads suffer from a variety of electro-mechanical related problems which affect laser scanning performance. These include wobble, jitter, wear, windage and synchronization issues. A novel optical structure consisting of two concentric and cylindrical interfaces with unique optical coating properties for the static projection of a laser spot array over a wide angle is demonstrated. The resulting ray trajectory through the waveguide is modeled using linear equations. Spot size growth is modeled using previously defined ray transfer matrices for tilted optical elements. The model is validated by comparison with experimental spot size measurements for 20 transmitted beams. This novel form of spot projection can be used as the projection unit in optical sensing devices which range to multiple laser footprints.

OCIS codes: (280.3420) Laser sensors; (080.2740) Optical design; (080.2730) Matrix methods

References and links

1. J. Besl "Active, Optical Range Imaging Sensors," Mach. Vision and Appl. **1**, 127-152 (1988).
2. F. Blais, "Review of 20 Years of Range Sensor Development," Electronic Imaging **13,** 231-240 (2004).
3. G. Stutz, "Guiding Light," SPIE OE Magazine **5,** 25-27 (2005).
4. A. B. Colquhoun, D. W. Cowan, and J. Shepherd "Trade-offs in rotary mirror scanner design," Proc. SPIE **1454,** 12-19 (1991).
5. G. A. Massey and A. E. Siegman, "Reflection and Refraction of Gaussian Light Beams at Tilted Ellipsoidal Surfaces," Appl. Opt. **8,** 975-978 (1969).
6. B. E. A. Saleh and M. C. Teich, *Fundamentals Of Photonics* (Wiley-Interscience, 1991).
7. H. Kogelnik and T. Li, "Laser Beams and Resonators," Appl. Opt. **10,** 1550-1567 (1966).

1. Introduction

Active, optical ranging devices can employ several broad techniques to derive depth information for a single point of interest on the object's surface. Generally, laser radar (LaDAR) uses pulsed time-of-flight or continuous-wave frequency or amplitude modulation to measure distance. Modes of triangulation use trigonometry, taking into account the baseline distance between the sensor and emitter, the projection angle, the focal length and the sub-pixel position of the spot's peak intensity [1,2].

In order to extend to a 2D profile, or 3D area measurement, one must project a pattern of structured light or a sequence of laser beams onto the object covering many points of interest. The stability and accuracy of the light projection unit is one of the crucial factors for scanner performance. Conventional LaDAR scanners rotate or oscillate the scanner unit at very high speeds or by employing a system of rotating mirrors that deflect a single incident beam in many directions to cover a wide angle.

#79773 - $15.00 USD Received 7 February 2007; revised 8 March 2007; accepted 9 March 2007

The problems encountered in polygonal-mirror and servo-motor-based scanners are mainly caused by moving parts, which can attain rotation speeds in the order of 1000 rpm. Angular deviation from the desired optical path and jitter are caused by mounting errors, random ball bearing wobble, motor cogging and torque variations. Motor stability and durability is also an issue. There is an upper limit to the rotation speed due to tensile strength of the mirror material which must not disintegrate at the maximum rotation speed. Synchronization with other time-dependent elements in the system can also be difficult. Furthermore, warm up time can be an issue [3, 4].

This paper proposes a novel approach that eliminates these common electro-mechanical related scanning problems. This approach is based on the use of a cylindrical quasi-cavity that generates a laser spot pattern over a wide angle through multiple beam reflections and partial transmission. A quasi optical cavity formed by two coated curved dielectric interfaces enclosing a transparent solid medium is modeled and experimentally demonstrated for wide angle spot generation. Ray trajectory both within the cavity and transmitted rays from the outer interface is analytically simulated using ray optics, and spot size growth is theoretically predicted using ray transfer matrix methods for off-axis optical systems [5]. Measured beam trajectory and spot size results show excellent agreement with the theoretical prediction.

2. Methods and materials

2.1 Quasi-cavity properties

The behavior of rays within resonators, resonator configurations and their modes are well known [6, 7]. In the case of this research, the presented optical component is cylindrical, does not substitute a paraxial optical system and does not contain resonant modes. Also, since it is not being used in the context of laser gain and a novel application is being researched, from hereafter it will be referred to as a quasi-cavity.

The custom fabricated concentric concave-convex cavity structure is shown in Fig. 1. It comprises an inner interface and outer interface of radii R_1 and R_2, respectively, separated by a BK-7 glass medium of thickness $d = R_2\text{-}R_1$, and entrance and exit windows. Light transmission is achieved by depositing nano-layered thin film coatings on both interfaces. The rear side is deposited with a highly reflective coating (R≥99%) and the front side with a partial transmission coating (T≤13%), both effective over the 600 – 900nm waveband. Hence, at every reflection with the outer interface, a fraction of the light is transmitted through the cavity thus generating a laser spot. The reflected power undergoes further reflections within the cavity to generate subsequent laser spots as described in the next subsection.

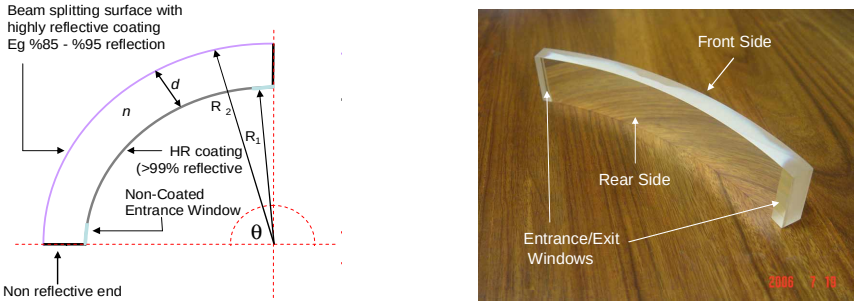

(a) (b)

Fig. 1. The novel optical quasi-cavity. (a) shows a top view schematic where $\theta_c = 90°$ and (b) is a photo of the fabricated product where $\theta_c = 45°$.

#79773 - $15.00 USD Received 7 February 2007; revised 8 March 2007; accepted 9 March 2007

2.2 Ray tracing

Figures 2 and 3 illustrate the ray propagation within and outside the cavity. It is noted that the rays propagating between the quasi-cavity interfaces are not paraxial and do not share a common optical axis. Therefore, the use of ray transfer matrices based on periodic optical systems is not a feasible method in terms of determining a new distance from the optical axis and new inclination at the output plane after every reflection.

To trace the path of the reflected and transmitted rays, optical geometry is used with no approximation. Given the radii of curvature of the two interfaces, the slope and ray intercept with the inner interface, the two surfaces and rays are modeled using a system of basic linear equations. Rays are plotted as straight lines, given by

$$y = mz + b, \tag{1}$$

where m is the gradient and b is the y-intercept. The two interfaces are plotted as arcs where

$$y = \sqrt{R_n^2 - z^2}, \tag{2}$$

where R is the interface radius and n corresponds to interface 1 or 2.

Intersections between rays and the surfaces are represented by algebraic solutions to Eqs. (1) and (2). Internal interfaces are modeled as cylindrical mirrors, hence the incidence and reflection angles of a ray are equal. Plots in the z-y coordinate plane illustrating the ray trace for a 90°-cavity are shown in Figs. 2 and 3 for R_1=0.25m and R_2=0.263m.

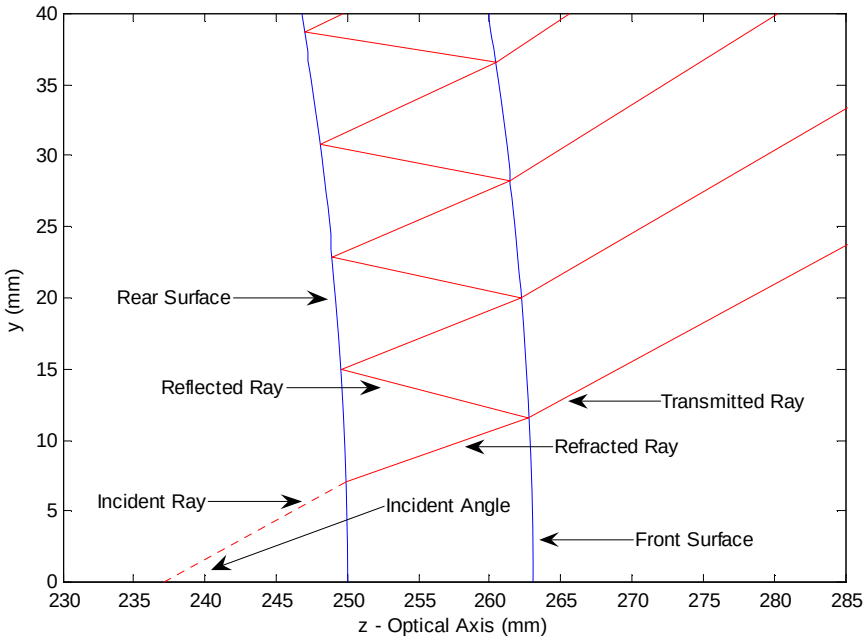

Fig. 2. Modeling of the ray trajectory showing a close up of the incident ray and the resulting refracted, transmitted and reflected rays.

#79773 - $15.00 USD Received 7 February 2007; revised 8 March 2007; accepted 9 March 2007

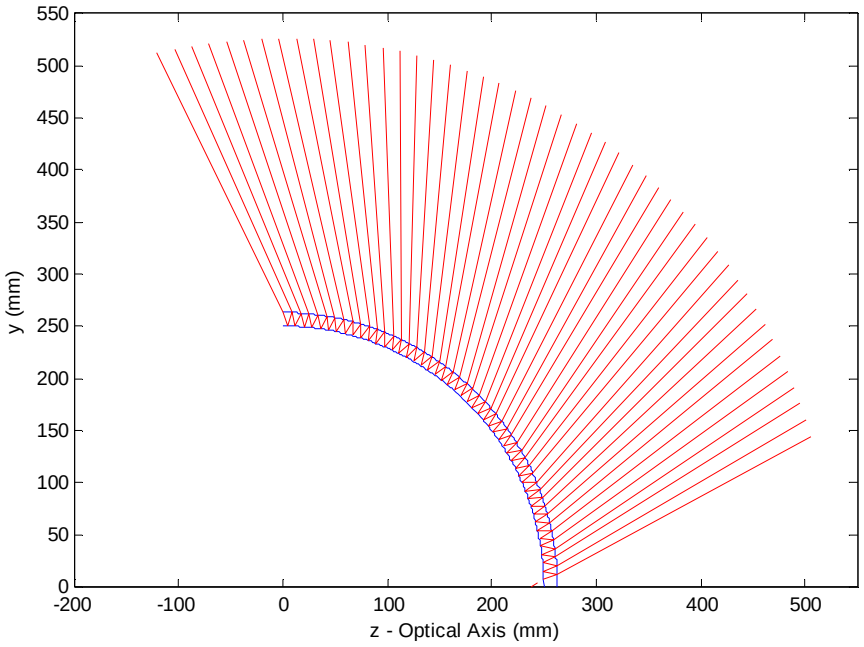

Fig. 3. Modeling of the ray trajectory showing the generated fan of rays from a quasi-cavity of 90° curvature.

2.3 Gaussian modeling

The effect of multiple internal reflections and refractions is analyzed using the Gaussian complex radius of curvature, *q*, in conjunction with ABCD transfer matrices [6]. Both the curvature of the wave front, *R*, and the spot radius of the beam, *W*, are functions of the propagation distance *z* and the Rayleigh range z_R. These distances are described by the complex variable *q*, given by

$$q = z + iz_R \tag{3}$$

If the laser source is included as part of the optical system, *q* must be derived at the laser aperture, at the rear interface entrance window and after refraction through the entrance window. The output beam radius W_{out}, divergence angle θ_0 and wavelength λ of the laser producing the incident beam is used to calculate the propagation distance at the laser output aperture, z_R. First we obtain the waist radius W_0 using λ and θ_0.

$$W_0 = \frac{\lambda}{\pi\theta_0}. \tag{4}$$

Secondly, we obtain the Rayleigh range, z_R, using the previously derived W_0.

$$z_R = \frac{\pi W_0^{\,2}}{\lambda}. \tag{5}$$

#79773 - $15.00 USD Received 7 February 2007; revised 8 March 2007; accepted 9 March 2007

The position of the beam at the laser aperture relative to its waist can be calculated as follows [6]

$$z_{output} = z_R \left(\left(\frac{W_{out}}{W_0} \right)^2 - 1 \right)^{\frac{1}{2}}. \quad (6)$$

Next, the standard paraxial ray–transfer *ABCD* [6] matrices for free space propagation and refraction at a spherical boundary can be applied to derive q at the entrance window and after refraction through it, respectively.

Once q values at the laser output aperture, at the cavity window and after refraction through the cavity window are derived, calculation of q_n after n reflections is carried out through an iterative two-step process. Firstly, the transfer matrix for a beam propagating through a uniform medium length is used to evaluate the q value at an interface. Secondly, either the matrix for reflection or refraction is used to calculate the q values for the transmitted or reflected rays, respectively. This iterative process is described in Fig. 4.

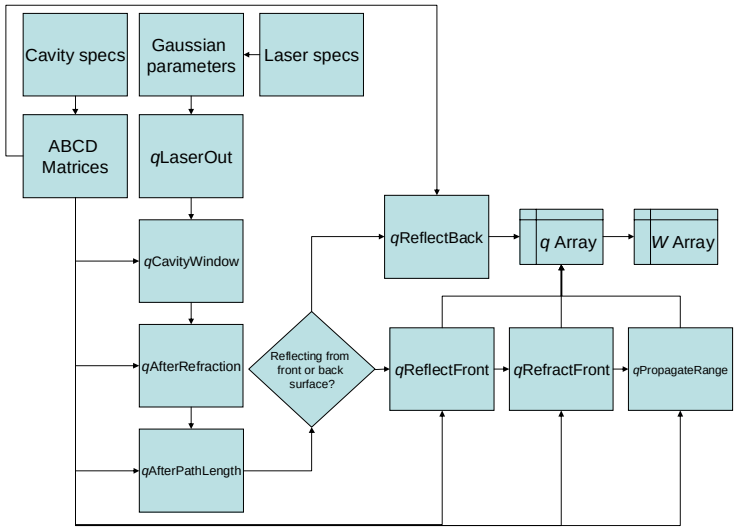

Fig. 4. Data flow diagram for determining q at various stages in the optical system, from the laser aperture to a projected range from the front interface.

To simulate the ray propagation in a cylindrical cavity, a new optical axis must be defined for each intersecting ray. Hence, *ABCD* matrices which incorporate coordinate transformation for reflection and refraction of a Gaussian laser beams at an off-axis ellipsoidal surface have been used as reported in [5].

Figure 5 shows simulated spot sizes upon reflections at the front and rear interfaces, as well as refraction at the front interface which negatively offsets the spot size. Figure 6 shows plots for the evolution of the spot diameter for 20 transmitted beams from the front interface of the quasi-cavity over a distance of 0.5m. At 0.5m, there is an increase in beam width from 1.22mm at the first spot to 2.81mm at the 20th beam.

By increasing the interface radii while maintaining a constant cavity thickness of 13mm, the spot size growth becomes smaller as shown in Fig. 7. When the cavity radii increase to R_1 = 1.053m and R_2= 1.063m, only an increase from 1.21mm to 1.64mm is seen over the 20 spots. This drop in spot size growth is the direct result of larger cavity radii.

#79773 - $15.00 USD Received 7 February 2007; revised 8 March 2007; accepted 9 March 2007

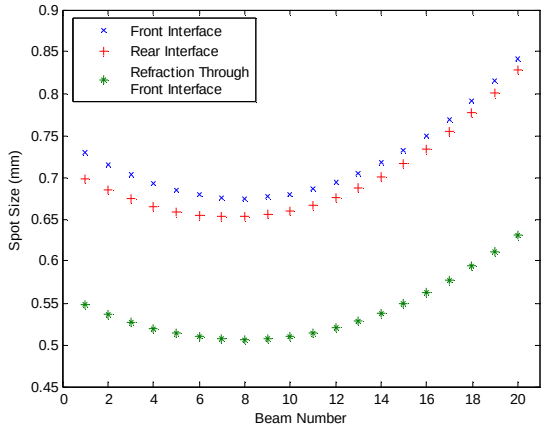

Fig. 5. Modeled spot sizes at reflections from the front and rear interfaces, and refraction at the front interface using non-paraxial *ABCD* matrices.

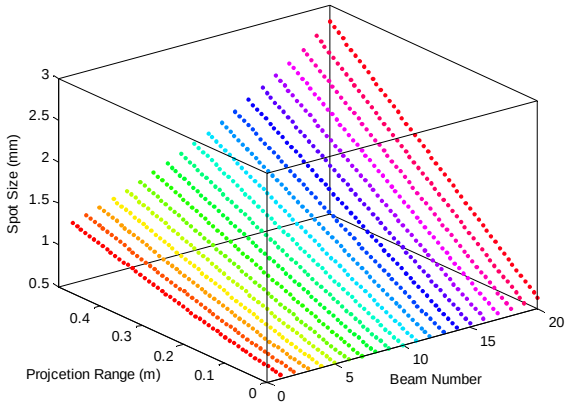

Fig. 6. Spot size evolution of transmitted beams over a half meter range using non-paraxial *ABCD* matrices, where R_1 = 0.25mm and R_2 = 0.263mm

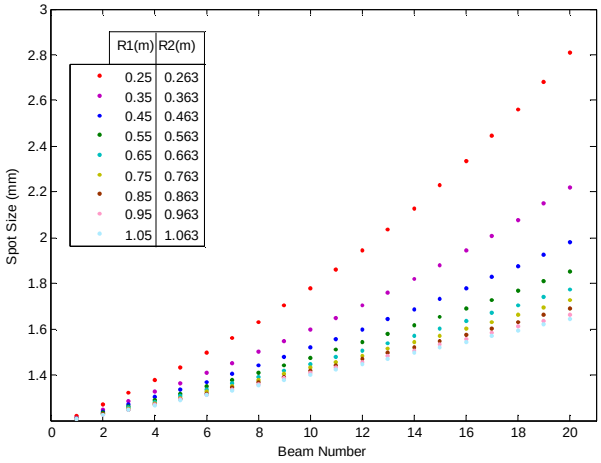

Fig. 7. Spot size growth rate decline with respect to an increase in interface radii. Spot sizes are modeled at a half meter range using non-paraxial *ABCD* matrices.

#79773 - $15.00 USD Received 7 February 2007; revised 8 March 2007; accepted 9 March 2007

2.4. Experimental setup for spot size measurements

A HeNe laser of 0.48mm output diameter and 1.7*m*rad divergence was used to produce a beam at an incident angle of 29° relative to the *z*-axis. The cavity radii were R_1 = 0.25m and R_2 = 0.263m. This generated 24 spots with the fabricated quasi-cavity described previously.

Spot size measurements were conducted using a near infrared camera with a 1 inch Vidicon image sensor. Since the quasi-cavity to camera distance was small enough to image one spot at a time without focusing, no lens system was necessary. Images from the 700 horizontal line camera were digitized in 8-bit resolution by a frame grabber installed on a personal computer with beam diagnostic software. Sixteen frames were acquired at a time for each of the first 20 spots and the mean used for the measurement value. A polarizer was placed in front of the laser aperture and rotated accordingly to avoid reaching the camera's damage threshold and saturation. The camera's manual analog gain was also adjusted to avoid any ambient noise. The beam measurement method chosen by software was the industry standard 90/10 knife edge method which is well suited for a TEM_{00} beam.

3. Measurement results and discussion

3.1 Spot size measurements

The measured and modeled spot size plots followed the same behavior in growth as shown in Fig. 8. It is important to notice that less than 10% discrepancy between theoretical and experimental data is demonstrated, which is attributed to measurement errors due to (i) the angle at which each laser beam was incident on the image sensor, (ii) varying sensitivity at different parts of the image sensor and (iii) the camera's gain factor which affected the intensity distribution of each spot. Also, the estimation of the position of the image sensor within the camera housing contributed to the overall discrepancy. This small discrepancy validates the theoretical model based on *ABCD* non-paraxial matrices, which is presented in section 2.C. Note that the beam width growth over the first 20 spots is considerable for the fabricated cavity, where the 20th spot measures double the diameter of the first spot. This is due to the non-focusing and compounded nature of the spot size growth where every change in spot size depends on the previous Gaussian complex parameter.

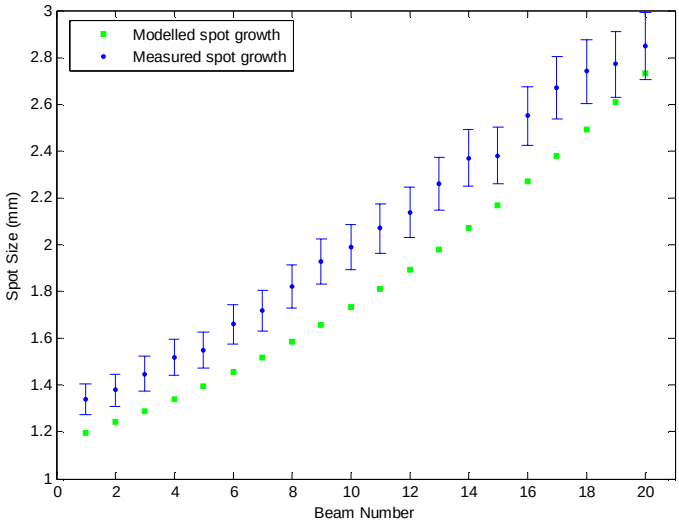

Fig. 8. Measured and modeled spot size growth for beams transmitted from the front side at a half meter range.

#79773 - $15.00 USD Received 7 February 2007; revised 8 March 2007; accepted 9 March 2007

3.2 Ray trajectory measurement

To validate the modeled ray trajectory described in section 2B, the intersecting coordinates of 20 rays with a vertical line plotted from (277,0) to (277,500) was recorded with the quasi-cavity center at (0,0) and R_1 = 0.25m and R_2 = 0.263m. Experimentally, a screen was placed in the same position relative to the cavity. The projected spot positions were marked on the screen and then measured with a ruler. The recorded *y* coordinates for the 20 intersections is compared to the measured positions. Figure 9 shows the modeled and measured positions along the screen. Position on screen refers to the distance from the spot to screen end (277,0).

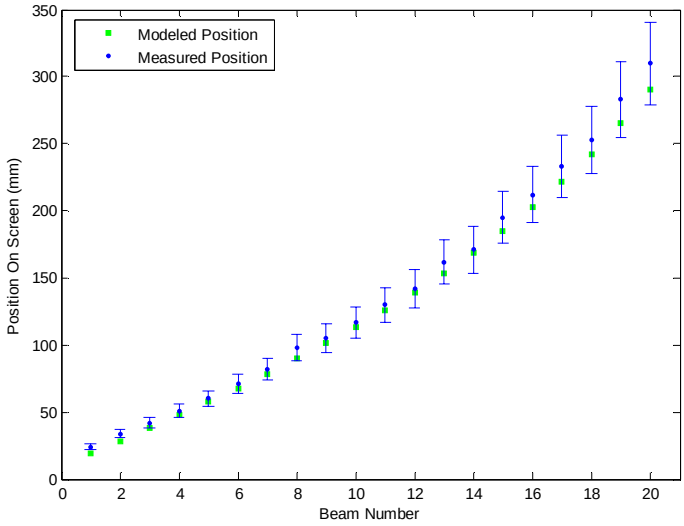

Fig. 9. Measured and modeled spot positions on screen.

A 0.7mm lead pacer was used to mark each spot, therefore a standard deviation of 10% has been applied. The difference in measured and modeled results begins to increase from the 15th spot. This is due to an increasingly larger angle each beam makes with the screen which results in a wider spot. Hence approximation of the spot center by hand becomes more difficult. However, Fig. 9 shows close conformity of the modeled and the approximately measured positions, therefore confirming the accuracy of the ray tracing method described previously.

4. Conclusions and future work

This paper has presented a novel method for wide angle pattern projection in the form of a laser spot array through multiple internal reflections and refractions. The effect of an off-axis optical system with respect to ray trajectory has been demonstrated. The wave guiding effect of the off-axis quasi-cavity on the spot size has also been successfully modeled and validated with experimental spot size measurements. The measured first and 20th spot sizes for a cavity of radii R_1 = 0.25m and R_2 = 0.263m have been 1.2mm and 2.8mm respectively. However, simulated results have shown that the 20th spot size can be reduced to only 1.6mm by increasing the cavity radii to R_1 = 1.05m and R_2 = 1.063m, thus improving the scanning quality.

Future work will include performing range measurements to each spot using dual triangulation and testing the performance of the ranging system, having the quasi-cavity as the emitting unit. A method for controlled spot projection also needs to be implemented.

By conjoining as many quasi-cavities as needed, the scanned angle can be extended to 360°. Furthermore, scanning in elevation can be achieved by stacking the quasi-cavities vertically.

#79773 - $15.00 USD Received 7 February 2007; revised 8 March 2007; accepted 9 March 2007